THE STRUCTURAL INVENTORY OF MID-SIZED COMPLEX IMPACT CRATERS FORMED IN SEDIMENTARY TARGETS. T. Kenkmann[1], [1]Institute for Earth and Environmental Sciences – Geology, Albert-Ludwigs-Universität Freiburg, Germany (Thomas.kenkmann@geologie.uni-freiburg.de).

Introduction: This abstract provides a review of the macro-scale structural inventory of mid-sized complex craters (5-15 km ∅) formed in sedimentary targets. The analysis is mainly based on terrestrial crater studies but also includes structural analysis of martian craters [1]. A comprehensive review is given in [2].

Crater rim: The crater rim of pristine complex craters usually shows a pronounced morphological elevation with a scarp at the inner side. The elevated rim is formed by the ejecta blanket plus uplifted bedrock. Recent analyses of complex lunar and martian craters indicate that target uplift plays the dominant role for the elevation. The circumferential crater rim escarpement is the outermost fault visible on the uneroded target surface and usually forms one of the major terrace steps in the crater rim region. On Earth, where the original morphology of craters is often barely visible and the ejecta blanket is removed, the outermost continuous concentric normal fault usually defines the final crater diameter of a complex impact crater. However, [3] stated that these outermost faults visible in eroded craters can lie further outwards than the main escarpments of uneroded structures. They suggest the terms "rim diameter" for uneroded craters and "apparent diameter" for eroded structures. The main faults are often associated with synthetic or antithetic faults. Pre-existing faults and joints can be reactivated during crater modification. Such craters often appear as polygonal craters with straight rim segments that run along the pre-existing joints [4]. Very deeply eroded impact structures are typically not defined by concentric normal faults. Instead circumferential monoclines or a combination of inward dipping normal faults and monoclines are common, particularly if the target is a sedimentary and stratified one (Fig. 1). The inner limb of a crater rim monocline usually dips downward towards the crater, and the crater rim can be defined by the trace of the monocline's hinge.

Crater moat: In pristine craters the moat between the crater rim and the central uplift is buried under a variety of breccias (talus breccias, crater floor breccias, air-borne breccias) as well as impact melt. Beneath this crater fill a complex ring syncline exist that is mostly asymmetric in radial cross section, with a steeply dipping or even overturned inner limb and a more gently dipping outer limb that is often segmented by normal faulting. The syncline is radially and concentrically subdivided into numerous fault-bounded segments or disintegrated into blocks. Between the crater rim and the axis of the ring syncline, normal faults of more or less concentric strike are frequent. Normal faulting along non-planar faults is commonly associated with antithetic or synthetic rotations of the hanging-wall unit. These faults often develop listric shapes. In stratified target rocks they can merge into low-angle detachments at depth (Fig. 1a) to compensate for the inward movement of material during crater collapse [5]. The presence of low-angle faults or detachments is favored by a large-scale rotational flow field that exists during crater collapse. It comprises uplift in the center and associated down-sagging in the periphery. Bedding planes of the stratified sediments are often used as glide planes. Displacements related to the modification stage commonly indicate inward and downward motion within the ring syncline. Due to the formation of the central uplift and passive rotation, the low-angle normal faults may transform into outward dipping thrust faults and reverse faults in the inner limb of the ring syncline [6]. The structural complexity of the ring syncline increases towards the center because the amount of lateral constriction increases by the motion of rock towards the center. The convergent particle trajectories during inward flow can be compensated either by a bulk thickening of inward sliding masses (tight folding, stacking of rock units along reverse faults, plastic flow) or by the formation of radial transpression zones (Fig. 1c). They develop at the edges of the obliquely converging rock masses during inward flow [7]. Different modes of uplift are possible, including lateral over-thrusting (Fig. 1b) and the formation of positive flower structures.

Central peaks: The intensity of deformation culminates within the central uplift. The deformation inventory of central uplifts is extremely complex and could be unraveled only for a few terrestrial impact craters with a sedimentary target. In the absence of appropriate marker beds, impacts into crystalline rock targets often do not allow the motions to be reconstructed in detail. Moreover, the absence of soft layers may prohibit folding in crystalline targets. Field analysis of a number of impact craters eroded to different levels and numerical modeling have proven that the centrally uplifted area becomes broader with depth while the observable stratigraphic uplift decreases [2]. Simultaneously, the diameter of the crater shrinks with depth. Both circumstances cause the increase of the ratio of the central uplift diameter to the apparent crater diameter with increasing depth of erosion. Consequently, the central uplift is by far the dominant

structural feature for deeply eroded craters; the moat and crater rim become faint features at depth.

Although each crater is unique complex impact craters up to 10-20 km formed in sedimentary targets show common features in their central uplift structure: anticlines and synclines with radial fold axes are typical for the periphery of central uplifts (Fig. 1d). They result from constriction caused by the convergent mass flow. Radial fold axes usually plunge outward and cause the serrated appearance of central uplifts. The hinge line of these radially striking folds is often bent and plunges more steeply with increasing proximity to the core of the central uplift. Near the center, vertical folds or folds with overturned hinges can develop [2]. Moreover, a gradational transition in fold tightness, wavelength, and amplitude may be detected, with open symmetrical anticlines of the central uplift periphery changing into isoclinal and overturned folds (Fig. 1e) towards the center. Spatial incompatibilities of the folds increase with increasing fold tightness. This leads to the initiation of reverse faults in the core of these folds and their rapid propagation into the limbs to finally offset one of the fold limbs from the other. As a consequence, fold limbs become detached into sheet-like blocks, bounded by reverse faults, which "stack up" against the core of the central uplift in an imbricated fashion (Fig. 1f). Fault-bounded blocks usually build up the core of a central uplift. In sedimentary targets, the stratigraphic context can be completely broken up. The occurrence of brecciation and breccia bodies is at first limited to the edges of blocks as fault breccias. They become the dominant rock type in the core of the central uplift. At a certain threshold diameter, central uplifts become gravitationally unstable and start to collapse under their own weight to form a morphological ring of peaks in pristine craters. Craters near the transition diameter show vertical flanks of their central uplifts. Localized kinking and buckle folding of the vertically uplifted strata indicate the onset of collapse [8]. Widespread overturning of strata in the central uplift periphery, e.g. [6], is one mechanism which enables the outward collapse. The overturning strata collide with the inward moving blocks of the surrounding ring syncline and form a complex interference zone [5]. The gravitational collapse also induces the development of normal faults dipping radially outward and offsetting the uplifted strata. Eventually, the collapsing central uplift flows outward, thereby overthrusting the downfaulted rocks of the surrounding ring syncline and forms a peak ring.

References: [1] Wulf, G. et al. (2012) Icarus 220, 194. [2] Kenkmann, T. et al. 2014. J. Struct. Geol. *in press.* [3] Turtle, E. P. et al. 2005. GSA SP 384, 1. [4] Eppler, D. T., et al. 1983. GSA Bull. 94, 274. [5] Kenkmann, T., et al. 2000. Lect. Not. Earth Sci., 91, 279. [6] Jahn, A., Riller, U., 2009. Tectonophys. 478, 221. [7] Kenkmann, T., von Dalwigk, I., 2000. MAPS 35, 1189. [8] Kenkmann et al. 2011. MAPS 46, 875

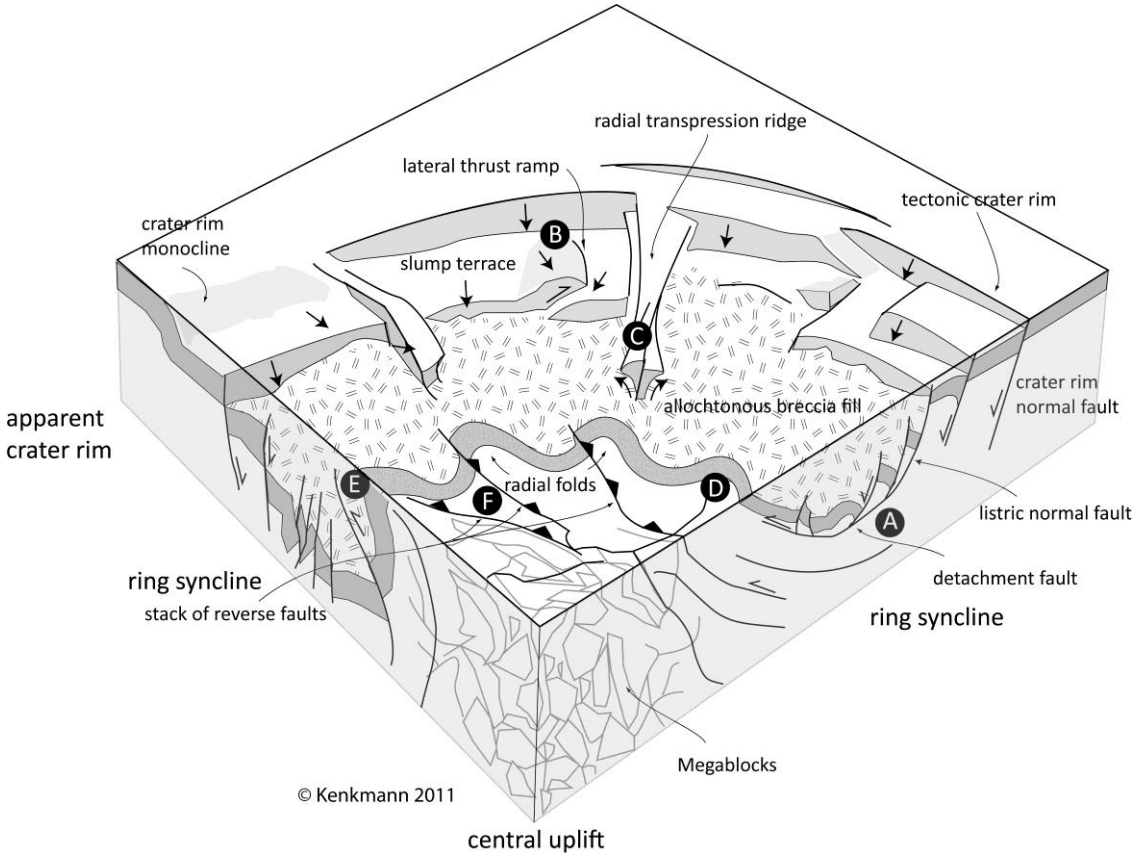

Fig. 2 Schematic block diagram illustrating the structural inventory and the locations of certain structures in the sub-surface of a complex impact crater.